

Original Article

Received Power Analysis of Visible Light LoS and NLoS System using Direct Detection

Sagupha Parween¹, Aruna Tripathy²

^{1,2}School of Electronic Sciences, Odisha University of Technology and Research, Odisha, India.

¹Corresponding Author : sagupha.parween@gmail.com

Received: 13 November 2024

Revised: 19 December 2024

Accepted: 09 January 2025

Published: 30 January 2025

Abstract - Optical wireless Communication (OWC) has emerged as a potential alternative to Radio Frequency (RF) technologies for high-speed indoor communication in recent years. An Indoor OWC, i.e. visible light communication (VLC) system, is investigated in this paper. The system operates similarly to optical fiber-based communication. However, the indoor wireless system uses a free space transmission medium rather than an optical fiber. In this paper, an indoor VLC system using a line of sight (LoS) and non-line of sight (NLoS) propagation model using direct detection has been designed. The channel impulse response and received power for LoS and NLoS systems are determined. The received power analysis has been carried out for different scenarios such as (i) single transmitter and single receiver in both LoS and NLoS systems, (ii) single transmitter and receiver in a hybrid (LoS and NLoS) channel condition where the power of LED has been split equally between LoS and NLoS paths, (iii) single transmitter and receiver in a hybrid system where the power of LED has been split unequally in LoS and NLoS paths, (iv) single transmitter and single receiver under four NLoS paths to show multiple reflections in the system, (v) two transmitters and single receiver in both LoS and NLoS paths, (vi) two transmitters and single receiver in a hybrid channel, (vii) single transmitter and two receivers in both LoS and NLoS channel, and the results are compared with the theoretical value.

Keywords - Visible light communication, Line of sight, Non-line of sight, Field of view, Received power.

1. Introduction

Visible light Communication (VLC) transmits data using white light-emitting diodes (LED), which flashlights at speeds that are imperceptible to the human eye [1]. High-speed connectivity and distortion-free usage anywhere are two significant advantages of VLC [2]. VLC system uses LED as the transmitter, which sends data at high speed which will be unnoticeable to the human eyes. The photodetector decodes the sent data after rapidly absorbing the light falling from the transmitter. The distinctive features of the VLC system, like license-free band features, straightforward implementation processes, and secure communication, all improve the use of the VLC system for a range of applications compared to the Radio Frequency (RF) communication system [2]. Because of this, VLC can be used for a wide range of applications like Indoor communications, transmitter and receiver positioning, vehicular communication, and underwater communication [3]. Many aspects need to be taken into account while creating a VLC system, such as high data rates, uplink problems, line of sight (LoS) / non-line of sight (NLoS) situations, range (the distance between transmitter and receiver), and interference. The LoS means Line of Sight. The propagation path in a LoS is defined as a direct path, i.e. there is no obstruction between the transmitter

and receiver during data transmission. In a non-line of sight (NLoS) path, there is no direct path between a transmitter and the receiver. Thus, a signal broadcast by the transmitter will encounter many reflections on its way to the receiver. The classification of indoor optical wireless communications networks is based on the degree of directionality (directed, non-directed, diffuse, and tracked) and the presence of a line-of-sight (LoS) channel between the transmitter and the receiver [4-7].

In literature [8], a VLC is implemented for LoS and NLoS systems considering only two scenarios, i.e. (a) a single transmitter and a single receiver and (b) two transmitters and one receiver. However, these represent very specific cases of a VLC system implementation. The proposed system has been designed and evaluated as a novel VLC system that consists of a single transmitter and two receivers in addition to the use of a reflector. In this work, unequal powers are allocated to the two receivers, which are different from the VLC systems reported in the literature. This division of the transmitted power is a novelty of this work, which was not attempted earlier. Moreover, in practice might need to implement a VLC system that makes use of multiple transmitters and multiple receivers in different



channel conditions. Therefore, a generic VLC system implementation using multiple transmitters and multiple receivers in both LoS and NLoS channel conditions is investigated here. The objective is also to evaluate the performance of the proposed system in terms of received power for the worst possible channel scenario. The channel considered here is also different from [8]. To show the NLoS scenario, [8] used an optical attenuator as a reflection from the wall, which had an attenuation value of 5 dB. However, the proposed work is different from [8] in the sense that a bidirectional reflector has been used where the actual reflectivity value can be varied from 0.1-0.8. This has been observed to provide a better channel model in terms of the reflections from the wall. In literature, VLC in the LoS channel has been designed in an OptiSystem simulator using the Free Space Optics (FSO) channel [9, 10]. The present paper uses a LoS channel, which is more practical in specifying the angle at which the transmitter transmits the signal and the angle at which the receiver receives the signal, which is not feasible in an FSO channel provided in the OptiSystem simulator. In [11], an investigation of received power was carried out by changing the semi-angle and distance between the transmitter and receiver using MATLAB. In this paper, the OptiSystem simulator has been used. Results obtained using the proposed system have been compared with [11]. It is found that the power received in the proposed system is better.

This paper also aims to investigate the received power for 10 different transmitter and receiver configurations under various LoS and NLoS scenarios. The 10 configurations so investigated are: (i) single transmitter and single receiver in a LoS channel, (ii) single transmitter and receiver in NLoS system, (iii) single transmitter and receiver in a hybrid (LoS and NLoS) system where power of LED has been split equally between LoS and NLoS paths, (iv) single transmitter and receiver in a hybrid (LoS and NLoS) scenario where power of the transmitter has been split and unequal powers in the NLoS path and the LoS path, (v) single transmitter and a single receiver in four NLoS paths to show multiple reflections in the proposed system, (vi) two transmitters transmitting the signal to a single receiver in a LoS channel, (vii) two transmitters transmitting the signal to a single receiver in a NLoS channel, (viii) two transmitters transmitting the signal to a single receiver under a hybrid channel condition where power of the transmitter has been split equally between LoS and NLoS paths, (ix) single transmitter transmitting to two different receivers in LoS system and (x) single transmitter transmitting to two different receivers in NLoS system. The proposed configurations in this paper have been tested for different scenarios of VLC systems. By implementing multi-transmitter, multi-receiver VLC systems, valuable insights into power received at each receiver are obtained for various channel conditions. The received power for different scenarios is compared with the

theoretical value and found to have a power difference of 0.056 dBm to 0.78 dBm.

2. System Model

2.1. LoS Propagation Model

Let us assume an indoor space is 10 m long, 10 m wide and 10 m high. A photodiode serves as the detector at the receiving point, while one LED acts as the transmitter, as shown in (Figure 1).

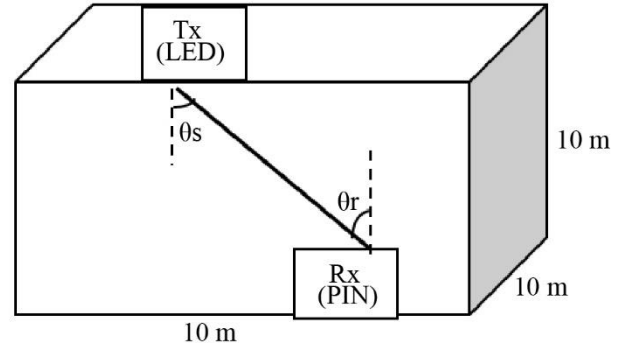


Fig. 1 LoS propagation model

Some of the studies assumed that a transmitter, especially an LED, is placed in parallel to a receiver [12]. Indoor positioning accuracy and dependability clearly decline if this assumption is incorrect.

When the transmitter and receiver are not positioned exactly parallel, the effects of tilting should be examined. Most VLC applications mainly use LED Lambertian radiation patterns at LoS conditions [13].

The angle at which the transmitter has transmitted the signal with respect to the normal is the irradiance angle, denoted by θ_s . The angle at which the receiver receives the signal with respect to the normal is said to be the incidence angle, and it is denoted by θ_r . The intensity at a certain angle θ is given by [14],

$$I(\theta) = I(0)\cos\theta \quad (1)$$

Where, $I(0)$ is the maximum intensity.

If the transmitter radiates at half-angle or semi-angle $\theta_{1/2}$, now the intensity is given as,

$$I(\theta_{1/2}) = \frac{I(0)}{2} = \cos^m \theta_{1/2} \quad (2)$$

A Lambertian distribution is characterized by its Lambertian order m . The Lambertian parameter m tells about the directionality of the radiation. A simplified version of Eq. (2) yields the Lambertian order m , which is given by [15],

$$\frac{I(\theta_{1/2})}{I(0)} = \frac{I(0)}{I(0)} \quad (3)$$

$$\cos^m \theta_{1/2} = \frac{1}{2} \quad (4)$$

$$\ln(\cos^m \theta_{1/2}) = \ln\left(\frac{1}{2}\right) \quad (5)$$

$$m * \ln(\cos \theta_{1/2}) = \ln\left(\frac{1}{2}\right) \quad (6)$$

$$m = \frac{-\ln(2)}{\ln(\cos \theta_{1/2})} \quad (7)$$

At the receiver, for VLC, it uses an optical concentrator before the PIN photodetector [16]. The signal reaches the concentrator with the incidence angle θ_r . Through the concentrator using total internal reflections the signal is received by the photodetector. The maximum angle to capture the signal at the optical concentrator is defined by field-of-view (FoV) denoted as φ_C . The concentration factor, i.e. gain of the optical concentrator, is given as [17],

$$g(\varphi) = \frac{n^2}{\sin^2(\varphi_C)} \quad (8)$$

The transmitted signal is multiplied by the channel impulse response before reaching the receiver. The frequency responses of optical channels can be used to determine the channel impulse response, i.e. optical DC gain, which connects the transmitted and received average powers. Optical channel model for the LoS condition, the channel dc gain or the channel impulse response $H_{LoS}(0)$ can be calculated as [18, 19],

$$H_{LoS}(0) = \frac{A_r(m+1)}{2\pi d^2} \cos(\theta_s) T_s g(\varphi_C) \cos(\theta_r) \quad (9)$$

Where A_r is the detection surface area, m is the Lambertian parameter, d is the distance between transmitter and receiver, θ_s and θ_r are the irradiance and incidence angle, respectively, T_s is the optical filter gain, and $g(\varphi_C)$ is the optical concentrator gain.

2.2. NLoS Propagation Model

Considering the same scenario of an indoor space, i.e. 10 m long, 10 m wide, and 10 m high, having a single transmitter and single receiver. The NLoS propagation model is shown in (Figure 2). The LED viewing angle is denoted by θ_s , and the light radiated by the transmitter. The light from the LED travels a certain distance before reflecting off the wall and arriving at the receiver at an angle θ_r . The angle of incidence to a reflective point and angle of irradiance to the photodetector is represented by the quantities α_i and β_r .

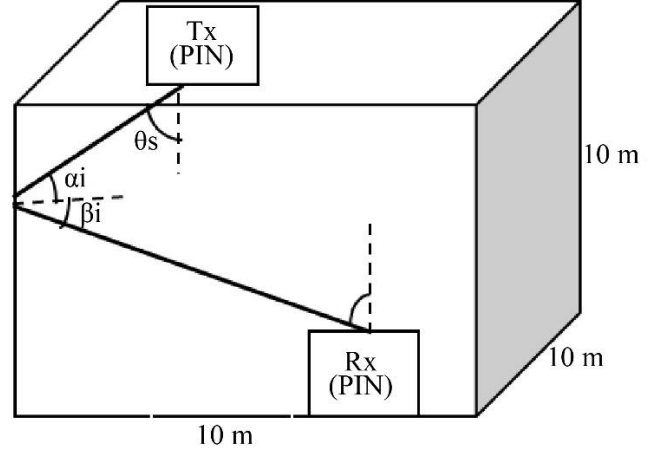


Fig. 2 NLoS propagation model

The channel impulse response $H_{LoS}(0)$ can be calculated as [20, 21],

$$H_{NLoS}(0) = \frac{A_r(m+1)\rho A_{wall}}{2(\pi d_1 d_2)^2} \cos(\theta_s) \cos(\alpha_i) T_s g(\varphi_C) \cos(\beta_r) \cos(\theta_r) \quad (10)$$

Where A_r is the detection surface area, m is the Lambertian parameter, d_1 is the distance between the transmitter and reflection point, d_2 is the distance between the reflection point and the receiver, θ_s and θ_r are the irradiance and incidence angle, respectively, α_i is the angle of incidence to a reflective point, β_r angle of irradiance to the photodetector, ρ is the reflection coefficient, A_{wall} is the reflective area of small region, T_s is the optical filter gain and $g(\varphi_C)$ is the optical concentrator gain. The received power after optical concentrator for LoS and NLoS system is given as [22]

$$P_r = P_t H_{LoS}(0) \quad (11)$$

$$P_r = P_t H_{NLoS}(0) \quad (12)$$

3. Proposed System

The schematic of the LoS propagation model is shown in (Figure. 3). Table 1 shows the components specification used for simulation. The simulation model uses a user-defined data sequence of 10 bits given as “1001101010” as transmitted data with a bit rate of 2.5×10^9 bits/s. The generated data is converted to NRZ electrical pulses, and these signals are transmitted through the LED. As the VLC use the range of wavelength from 400nm to 700nm, an LED of 550nm has been used for the simulation. The transmitter and the receiver are connected through the LoS channel. The FSO channel has been used in the literature to define the line-of-sight condition for a VLC LoS system. However, in the proposed scheme, a LoS channel has been used as specified in the OptiSystem simulator, which is more accessible to provide different input parameters for the VLC system, like

transmitter semi-angle, incident angle, and irradiance angle. At the receiving end, a PIN photodiode is used as the detector, which converts the optical signal to an electrical signal, and a low-pass rectangular filter filters out the detected electrical signal from the photodiode. A 3R regenerator is used for reamplification, reshaping and retiming of the received signal. Further, an oscilloscope visualizer compares the transmitted and receiver bits.

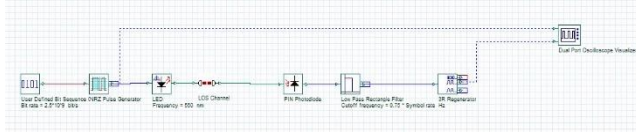


Fig. 3 Schematic layout of LoS propagation model

Table 1. Components specification for LoS system

Components	Parameters and their values
LED	Frequency: 550 nm
User Defined Bit Sequence Generator	Input bits: 1001101010 Bit rate: 2.5 x10 ⁹ bits/s
LoS Channel	Transmitter Semi angle=600 Irradiance angle= 200 Incidence angle= 00 to 890 Detection surface area: 1.5 cm ² Optical concentration factor: 2 Index concentration factor: 1.5 Link length= 10 m
PIN Photodetector	Material type: Silicon Responsivity: 1 A/W Dark current: 10 nA Absolute temperature: 298 K Load resistance: 50Ω Shot noise distribution: Gaussian Modulation bandwidth: 2 GHz Center frequency 193.1 THz

With the exception of taking the reflection point into account, this NLoS model is comparable to the LOS propagation model. In the literature, an optical attenuator has been used as a reflection from the wall, but the proposed system has used a bidirectional reflector as a reflection point. The bidirectional reflector will reflect the light coming from

the input depending on the reflection coefficient. It operates in a bidirectional manner, meaning the input signal can be applied in either direction and receives an appropriate output. If only one reflector in one direction is used for input, then the input from the other reflector in the opposite direction has been cancelled out using an optical null. The NLoS system is also tested for multiple reflections for the same composed room using a power splitter at the transmitter and a power combiner at the receiver end. The proposed system had considered three numbers of reflections. Here, a single LED is used, and the output signal from the transmitter is fed to 1x3 power splitters with equal power distribution in each branch, which further transmits the signal through three NLoS channels. The power at each branch of the 1 x N power splitter has been calculated as:

$$P_{oi} = \frac{P_i}{N} \tag{13}$$

$$P_{oi} (dBm) = P_i (dBm) - 10 \log(N) \tag{14}$$

Where P_{oi} is the power at each branch, $i=1,2,3,\dots$, P_i is the power of the incident light source, and N is the total no. of output port of the power splitter.

All three signals travel through different lengths and face the reflection. The three different bidirectional reflectors are used as a reflection point. After reflection, these signals travel through different lengths and reach the receiver again. The power combiner will sum up the power in each branch and send it to the receiver. At the receiving end, the PIN photodiode, a low-pass rectangular filter, 3R regenerator and oscilloscope visualizer to retrieve the transmitted signal. For a hybrid VLC system which contains both LoS and NLoS paths, the power splitter has been used to investigate the scenarios with different power splitting ratios in both paths. As the NLoS path faces many reflections so, more power should be required to send the data in comparison to the LoS path. The schematic layout for the NLoS system for single reflection and multiple reflections (i.e. three) is shown in (Figure. 4) and (Figure. 5) respectively.

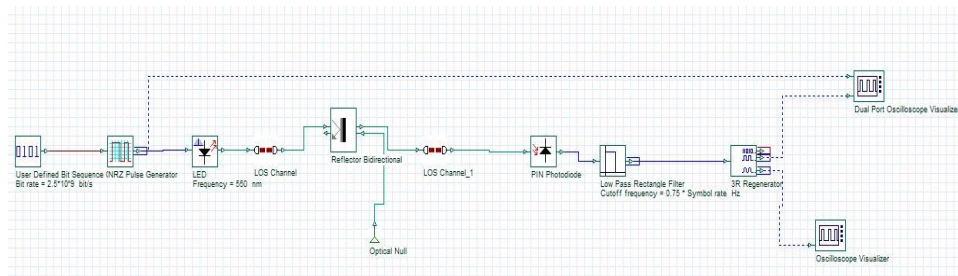


Fig. 4 Layout of NLoS Propagation Model for Single Reflection

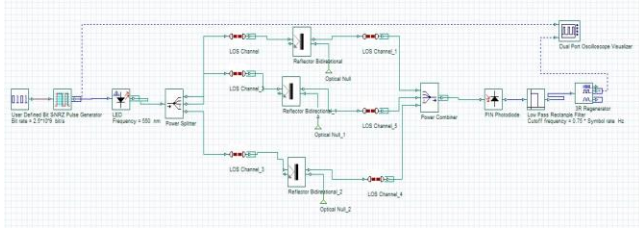


Fig. 5 Layout of NLoS propagation model for three reflections

Tables 2 and 3 show the component specifications used for simulation for the NLoS system for single reflection and the NLoS system for three reflections.

4. Results and Analysis

The OptiSystem simulation result of the propagation models is shown in Figure 6. The oscilloscope visualizer generates the input signal from the transmitter side and the output signal at the receiver.

Table 2. Components specification for NLoS system with a single reflection

Components	Parameters and their values
LED	Frequency: 550 nm
User Defined Bit Sequence Generator	Input bits: 1001101010 Bit rate: 2.5×10^9 bits/s
LoS Channel	Transmitter Semi angle=600 Irradiance angle= 200 Incidence angle= 00 to 890 Detection surface area: 1 cm ² Optical concentration factor: 2 Index concentration factor: 1.5 Link length= 5 m and 10m
Bidirectional Reflector	Reflection=50%
PIN Photodetector	Material type: Silicon Responsivity: 1 A/W Dark current: 10 nA Absolute temperature: 298 K Load resistance: 50Ω Shot noise distribution: Gaussian Modulation bandwidth: 2 GHz Center frequency 193.1 THz

Table 3. Components specification for NLoS system with three reflections

Components	Parameters and their values
LED	Frequency: 550 nm
User Defined Bit Sequence Generator	Input bits: 1001101010 Bit rate: 2.5×10^9 bits/s
LoS Channel	Transmitter Semi angle=600 Detection surface area: 1 cm ² Optical concentration factor: 2 Index concentration factor: 1.5 Link length (Channel-1)= 10 m and 5m Link length (Channel-2)= 5 m and 10m Link length (Channel-3)= 8 m and 4m
Bidirectional Reflector	Reflection=50%
PIN Photodetector	Material type: Silicon Responsivity: 1 A/W Dark current: 10 nA Absolute temperature: 298 K Load resistance: 50Ω Shot noise distribution: Gaussian Modulation bandwidth: 2 GHz Center frequency 193.1 THz

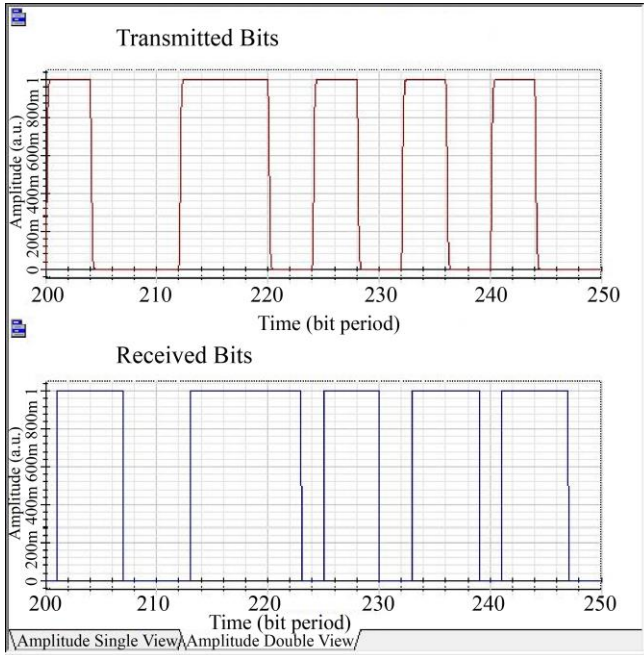


Fig. 6 Transmitted and received bits for LoS/NLoS propagation model

The comparison of the simulated and theoretical value of received power for LoS and NLoS systems is shown in Figures 7 and 8, respectively. Simulation parameters are set to find the received power in the LoS system as follows: the irradiance angle is kept at a constant angle of 20° , and the incidence angle is varied from 0° to 89° for the distance between the transmitter and receiver $d=10m$. For the NLoS system with single reflection, the parameters are set to $d_1=5m$ is the distance between the transmitter and reflection point, $d_2=10m$ is the distance between the reflection point and the receiver, $\theta_s=30^\circ$, $\alpha_i=40^\circ$, $\beta_r=60^\circ$ and θ_r is varied from 0° to 89° . $\rho=0.5$, $A_{wall}=0.01cm^2$, $T_s=1$, and $g(\varphi_C)=3$.

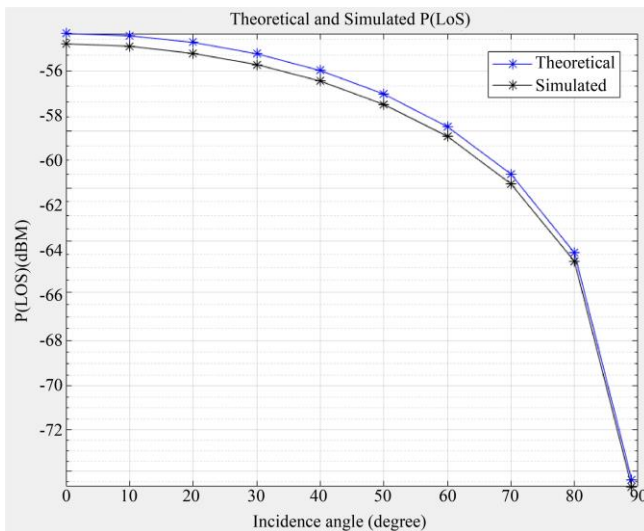


Fig. 7 Comparison plot for Received power for LoS System vs. Incidence angle

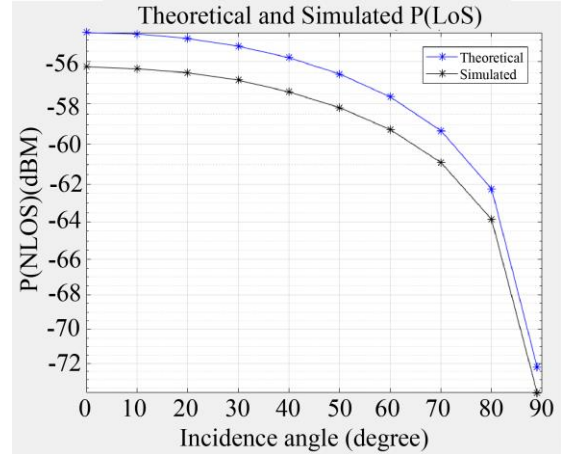


Fig. 8 Comparison plot for Received power for NLoS System with single reflection vs. Incidence angle

A comparison is made between [11] and the proposed work using the same input simulation parameters for a VLC LoS system. The comparison is based on two scenarios: (a) by varying the semi-angle from 15° to 90° , and (b) by varying the distance between the transmitter and receiver from 0.5m to 3m. The distance between the transmitter and receiver is the link distance. The comparison plot for both scenarios is shown in Figures 9 and 10, respectively. The proposed system performance is better than the [11].

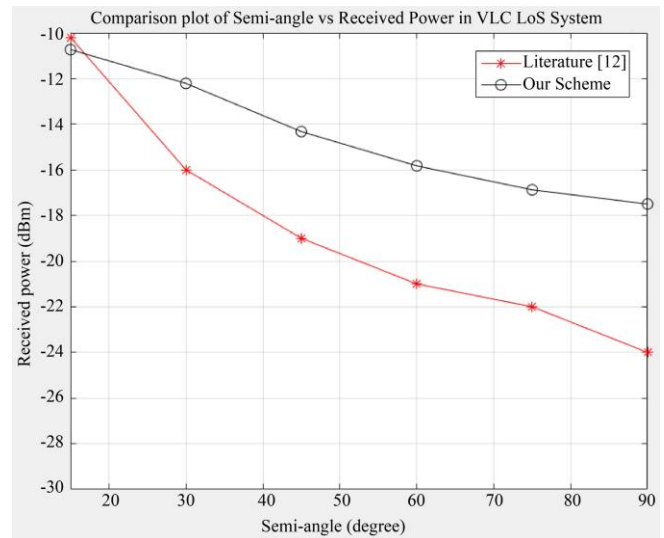


Fig. 9 Semi-angle vs. Received power

Different scenarios have been tested for the VLC LoS and NLoS system, and its theoretical and simulated received power has been computed. The comparison of theoretical and simulated received powers for various VLC indoor communication scenarios is presented in Table 4. Whether comparing a pure LoS system, a pure NLoS system or a hybrid system, the power difference in Figure 11 demonstrates that the simulated NLoS system experiences greater error than the LoS system.

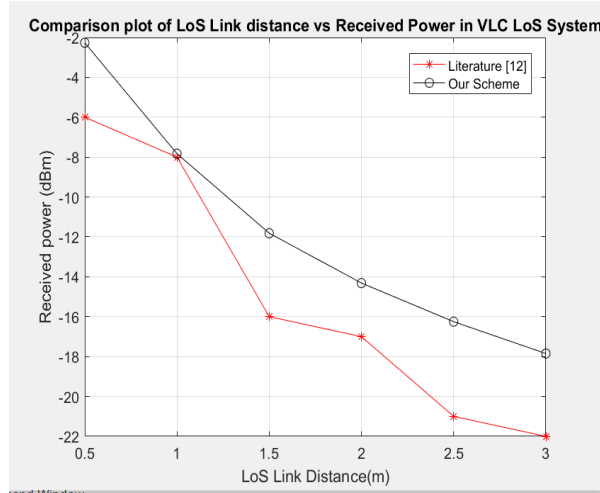


Fig. 10 Link distance vs. Received power

Table 4. Received power analysis for VLC system in different scenarios

Scenario	Input Simulation Parameters	Received Power (Theoretical) in dBm	Received Power (Simulated) in dBm	Power Difference in dBm	% Error
1 Tx and 1 Rx Single Path (LoS)	$P_{LED}=23.42$ dBm, $d=10$ m, $A_{wall}=0.01$ cm ² $\theta_{1/2}=60^\circ$, $\theta_s=30^\circ$, $\theta_r=20^\circ$, $T_s=1$, $g(\varphi_C)=2$	-29.43	-29.5	0.07	0.23
1 Tx and 1 Rx Single Path (NLoS)	$P_{LED}=21.132$ dBm, $d_1=5$ m, $d_2=10$ m, $\theta_{1/2}=60^\circ$, $\theta_s=30^\circ$, $\alpha_i=40^\circ$, $\beta_r=60^\circ$, $\theta_r=30^\circ$, $\rho=0.5$, $A_{wall}=0.01$ cm ² , $T_s=1$, $g(\varphi_C)=3$	-88.20	-88.816	0.616	0.7
1 Tx and 1 Rx Path1=LoS Path2=NLoS	$P_{LED}=22.832$ dBm, Power splitting ratio Path1=50%, and Path2=50%, $A_{wall}=0.01$ cm ² , $T_s=1$, $g(\varphi_C)=3$ Path1 LoS: : $P_{LoS}=19.822$ dBm, $d=10$ m, $\theta_{1/2}=60^\circ$, $\theta_s=20^\circ$, $\theta_r=30^\circ$ Path2 NLoS: : $P_{NLoS}=19.822$ dBm, $d_1=5$ m, $d_2=8$ m, $\theta_{1/2}=60^\circ$, $\theta_s=25^\circ$, $\alpha_i=40^\circ$, $\beta_r=30^\circ$, $\theta_r=40^\circ$, $\rho=0.5$,	Path1=-33.03 Path2=-85.52	Path1=-33.07 Path2=-85.9	Path1=0.04 Path2=0.38	Path1=0.12 Path2=0.44
1 Tx and 1 Rx Path1=LoS Path2=NLoS	$P_{LED}=22.832$ dBm, Power splitting ratio Path1=25%, and Path2=75%, A_{wall}	Path1=-36.04 Path2=-83.77	Path1=-36.31 Path2=-84.52	Path1=0.27 Path2=0.52	Path1=0.75 Path2=0.89

	$=0.01\text{cm}^2$, $T_s = 1$, $g(\varphi_C) = 2$ Path1 LoS: $P_{\text{LoS}}=16.807$ dBm, $d=10\text{m}$, $\theta_{1/2}=60^\circ$, $\theta_s = 20^\circ$, $\theta_r=30^\circ$ Path2 NLoS: $P_{\text{NLoS}}=21.58$ dBm, $d_1=5\text{m}$, $d_2=8\text{m}$, $\theta_{1/2}=60^\circ$, $\theta_s = 25^\circ$, $\alpha_i = 40^\circ$, $\beta_r=30^\circ$, $\theta_r=40^\circ$, $\rho=0.5$				
1 Tx and 1 Rx Four (NLoS) Path	$P_{\text{LED}}=22.832$ dBm, Power splitting ratio Path1=25%, Path2=25%, Path3=25%, Path4=25%, $P_{\text{NLoS}}=15.099$ (each), $A_{\text{wall}} = 0.01\text{cm}^2$, $T_s = 1$, $g(\varphi_C) = 2$ Path1 NLoS: $d_1=5\text{m}$, $d_2=10\text{m}$, $\theta_{1/2}=60^\circ$, $\theta_s = 30^\circ$, $\alpha_i = 40^\circ$, $\beta_r=60^\circ$, $\theta_r=30^\circ$, $\rho=0.6$ Path2 NLoS: $d_1=8\text{m}$, $d_2=4\text{m}$, $\theta_{1/2}=60^\circ$, $\theta_s = 30^\circ$, $\alpha_i = 60^\circ$, $\beta_r=45^\circ$, $\theta_r=35^\circ$, $\rho=0.5$ Path3 NLoS: $d_1=4\text{m}$, $d_2=8\text{m}$, $\theta_{1/2}=60^\circ$, $\theta_s = 30^\circ$, $\alpha_i = 50^\circ$, $\beta_r=20^\circ$, $\theta_r=30^\circ$, $\rho=0.4$ Path4 NLoS: $d_1=5\text{m}$, $d_2=6\text{m}$, $\theta_{1/2}=60^\circ$, $\theta_s = 40^\circ$, $\alpha_i = 10^\circ$, $\beta_r=45^\circ$, $\theta_r=35^\circ$, $\rho=0.7$	Path1=-92.19 Path2=-90.16 Path3=-89.35 Path4=-86.52	Path1=-92.97 Path2=-89.83 Path1=-89.46 Path2=-85.6	Path1=0.78 Path2=0.33 Path3=0.11 Path4=0.92	Path1=0.84 Path2=0.36 Path3=0.12 Path4=1.06
2 Tx and 1 Rx (LoS)	$P_{\text{LED}}=21.328$ dBm (Path1 and Path2), $T_s=1$, $g(\varphi_C)=2$ Path1 LoS: $d=10\text{m}$, $\theta_{1/2}=60^\circ$, $\theta_s=30^\circ$, $\theta_r=45^\circ$ Path1 LoS: $d=5\text{m}$, $\theta_{1/2}=60^\circ$, $\theta_s=30^\circ$, $\theta_r=20^\circ$	Path1=-32.76 Path2=-25.5	Path1=-33 Path2=-25.6	Path1=0.23 Path2=0.09	Path1=0.7 Path2=0.35
2 Tx and 1 Rx (NLoS)	$P_{\text{LED}}=21.313$ dBm (Path1 and Path2), $A_{\text{wall}} = 0.01\text{cm}^2$, $T_s=1$, $g(\varphi_C)=2$ Path1 NLoS: $d_1=5\text{m}$, $d_2=8\text{m}$, $\theta_{1/2}=60^\circ$, $\theta_s = 30^\circ$, $\alpha_i = 45^\circ$, $\beta_r=20^\circ$, $\theta_r=20^\circ$, $\rho=0.5$ Path2 NLoS: $d_1=4\text{m}$, $d_2=6\text{m}$, $\theta_{1/2}=60^\circ$, $\theta_s = 30^\circ$, $\alpha_i = 40^\circ$, $\beta_r=25^\circ$, $\theta_r=55^\circ$, $\rho=0.6$	Path1=-81.58 Path2=-78.3	Path1=-81.83 Path2=-77.72	Path1=0.25 Path2=0.58	Path1=0.3 Path2=0.74
2 Tx and 1 Rx Path1=LoS Path2=NLoS	$P_{\text{LED}}=21.327$ dBm (Path1 and Path2), $A_{\text{wall}} = 0.01\text{cm}^2$, $T_s = 1$, $g(\varphi_C) = 2$ Path1 LoS: $d=5\text{m}$,	Path1=-26.74 Path2=-80.05	Path1=-26.8 Path2=-80.72	Path1=0.056 Path2=0.66	Path1=0.2 Path2=0.82

	$\theta_{1/2}=60^\circ, \theta_s =30^\circ, \theta_r=45^\circ$ Path2 NLoS: $d_1=4m,$ $d_2=6m, \theta_{1/2}=60^\circ, \theta_s =30^\circ,$ $\alpha_i =40^\circ, \beta_r=25^\circ, \theta_r=55^\circ,$ $\rho=0.6$				
1 Tx and 2 Rx (LoS)	$P_{LED}=22.81$ dBm, Power splitting ratio Path1=50%, and Path2=50%, $P_{LoS}=19.8$ dBm (each), $T_s =1, g(\varphi_C) =2$ Path1 LoS : $d=10m,$ $\theta_{1/2}=60^\circ, \theta_s =30^\circ, \theta_r=45^\circ$ Path2 LoS : $d=10m,$ $\theta_{1/2}=60^\circ, \theta_s =45^\circ, \theta_r=45^\circ$	Path2=-34.29 Path2=-33.93	Path1=-34.3 Path2=-34.3	Path1=0.09 Path2=0.26	Path1=0.26 Path2=0.76
1 Tx and 2 Rx (NLoS)	$P_{LED}=22.84$ dBm (Path1 and Path2), $P_{LoS}=19.8$ dBm (each), $A_{wall} =0.01$ cm ² , $T_s=1, g(\varphi_C)=2$ Path1 NLoS: $d_1=6m,$ $d_2=4m, \theta_{1/2}=60^\circ, \theta_s =60^\circ,$ $\alpha_i =30^\circ, \beta_r=30^\circ, \theta_r=50^\circ,$ $\rho=0.6$ Path2 NLoS: $d_1=5m,$ $d_2=5m, \theta_{1/2}=60^\circ, \theta_s =20^\circ,$ $\alpha_i =40^\circ, \beta_r=25^\circ, \theta_r=55^\circ,$ $\rho=0.4$	Path1=-83.11 Path2=-83.31	Path1=-83.7 Path2=-83.93	Path1=0.58 Path2=0.6	Path1=0.96 Path2=0.72

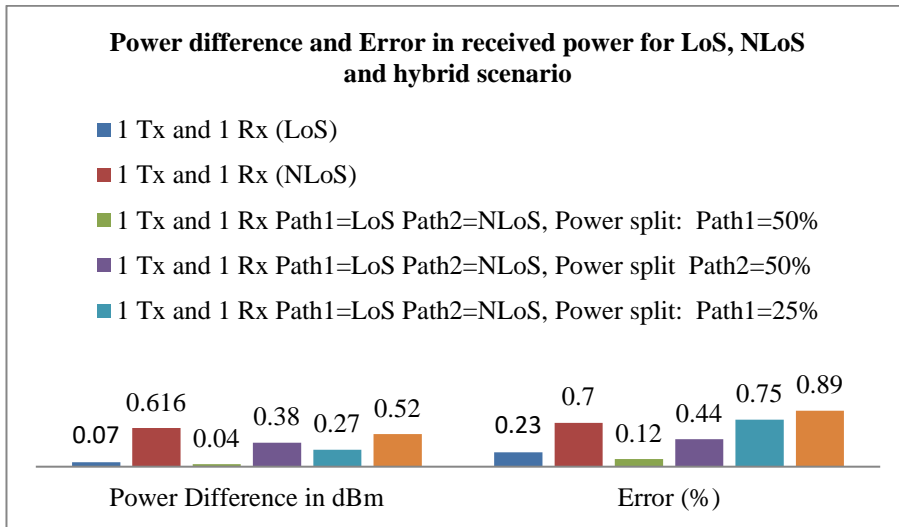


Fig. 11 Power difference and error in received power for LoS, NLoS and hybrid scenario

5. Conclusion

The experimental block schematic of indoor VLC has been implemented in OptiSystem 20.0, and all the simulation plots were done using MATLAB R2022a. The bar chart shows the power difference and error in received power for LoS, NLoS, and hybrid scenarios, which were implemented using Microsoft Excel 2010. For an indoor VLC system, the LoS and NLoS propagation models have been simulated.

The FoV for both LoS and NLoS systems is tested and found to be 90° , so it is better to keep all the angles below 90° . The simulated received power is compared with the theoretical value by varying the incident angle from 0° to 89° , and it is found that for smaller incidence angles, the received power has a difference of 1 dBm for the LoS system and 2 dBm for the NLoS system in comparison to the theoretical power. The received power analysis for the LoS system is also carried

out by varying the transmitter semi-angle and the link length. The received power decreases from -10.7 dBm to -18.5 dBm by increasing the transmitter semi-angle from 15^0 to 90^0 , which is also justified by Equations (8) and (9). By increasing the link length from 0.5 m to 3 m, the received power decreases from -2 dBm to -17.8 dBm. As the NLoS channel experiences reflections between the transmitter and the receiver, increasing the distance received power will be reduced. As shown in Equation (10), the distance d_1 and d_2 are inversely proportional to the $H_{NLoS}(0)$, so by increasing d_1 or d_2 , the $H_{NLoS}(0)$ will decrease, which will reduce the received power.

The proposed system also shows the power analysis received for different scenarios in a VLC system. The

received power difference between theoretical and simulated results has been computed, and it is found that the difference varies up to 0.33 dBm for the suggested LoS system, whereas for the NLoS system, the difference has been increased up to 0.78 dBm. Due to the reflection from the walls, the NLoS system faces more signal distortion than a LoS system. Future work may involve the implementation of the MIMO system model in VLC. Also, VLC can play an important role in IoT applications like smart lighting, home automation, e-healthcare, and industrial IoT. In smart lighting, the VLC network can provide high-speed communication through luminaries. In e-healthcare applications, the VLC network can provide reliable communication between medical devices. VLC systems used for IoT applications can be a future aspect to investigate.

References

- [1] Saif N. Ismail, and Muataz H. Salih, "A Review of Visible Light Communication (VLC) Technology," *2nd International Conference On Materials Engineering & Science (Iconmeas 2019)*, Baghdad, Iraq, vol. 2213, no. 1, 2020. [[CrossRef](#)] [[Google Scholar](#)] [[Publisher Link](#)]
- [2] Hongda Chen et al., "Advances and Prospects in Visible light Communications," *Journal of Semiconductors*, vol. 37, no. 1, pp. 1-10, 2016. [[CrossRef](#)] [[Google Scholar](#)] [[Publisher Link](#)]
- [3] Zuhang Geng et al., "Advances in Visible Light Communication Technologies and Applications," *Photonics*, vol. 9, no. 12, pp. 1-17, 2022. [[CrossRef](#)] [[Google Scholar](#)] [[Publisher Link](#)]
- [4] Penghua Lou et al., "Fundamental Analysis for Indoor Visible Light Positioning System," *2012 1st IEEE International Conference on Communications in China Workshops*, Beijing, China, pp. 59-63, 2012. [[CrossRef](#)] [[Google Scholar](#)] [[Publisher Link](#)]
- [5] J.M. Kahn, and J.R. Bany, "Wireless Infrared Communications," *Proceedings of the IEEE*, vol. 85, no. 2, pp. 265-298, 1997. [[CrossRef](#)] [[Google Scholar](#)] [[Publisher Link](#)]
- [6] C. Jenila, and R.K. Jeyachitra, "Green Indoor Optical Wireless Communication Systems: Pathway towards Pervasive Deployment," *Digital Communications and Networks*, vol. 7, no. 6, pp. 410-444, 2021. [[CrossRef](#)] [[Google Scholar](#)] [[Publisher Link](#)]
- [7] Nazmi A. Mohammed, and Mohammed Abd Elkarim, "Exploring the Effect of Diffuse Reflection on Indoor Localization Systems Based on RSSI-VLC," *Optics Express*, vol. 23, no. 16, pp. 20297-20313, 2015. [[CrossRef](#)] [[Google Scholar](#)] [[Publisher Link](#)]
- [8] Alwin Poullose, "Simulation of an Indoor Visible Light Communication System Using Optisystem," *Signals*, vol. 3, no. 4, pp. 765-793, 2022. [[CrossRef](#)] [[Google Scholar](#)] [[Publisher Link](#)]
- [9] Wei Xu et al., "Indoor Positioning for Multiphotodiode Device Using Visible-Light Communications," *IEEE Photonics Journals*, vol. 8, no. 1, pp. 1-11, 2015. [[CrossRef](#)] [[Google Scholar](#)] [[Publisher Link](#)]
- [10] Shivam et al., "Performance Analysis of an Indoor Visible Light Communication System Using Optisystem Software," *2023 Third International Conference on Advances in Electrical, Computing, Communication and Sustainable Technologies*, Bhilai, India, pp. 1-6, 2023. [[CrossRef](#)] [[Google Scholar](#)] [[Publisher Link](#)]
- [11] Adhytya Dhava Shalsa Putra et al., "Simulation of Visible Light Communication and Free Space Optic for IoT Using Optisystem," *2022 International Symposium on Electronics and Smart Devices*, Bandung, Indonesia, pp. 1-5, 2022. [[CrossRef](#)] [[Google Scholar](#)] [[Publisher Link](#)]
- [12] Syifaal Fuada, Angga Pratama Putra, and Trio Adiono, "Analysis of Received Power Characteristics of Commercial Photodiodes in Indoor Los Channel Visible Light Communication," *International Journal of Advanced Computer Science and Applications*, vol. 8, no. 7, pp. 164-172, 2017. [[CrossRef](#)] [[Google Scholar](#)] [[Publisher Link](#)]
- [13] Muhammad Towfiqur Rahman et al., "Review of Advanced Techniques for Multi-Gigabit Visible Light Communication," *IET Optoelectronics*, vol. 14, no. 6, pp. 359-373, 2020. [[CrossRef](#)] [[Google Scholar](#)] [[Publisher Link](#)]
- [14] Xiangyang Zhang et al., "Analysis of the Applicable Range of the Standard Lambertian Model to Describe the Reflection in Visible Light Communication," *Electronics*, vol. 11, no. 9, pp. 1-24, 2022. [[CrossRef](#)] [[Google Scholar](#)] [[Publisher Link](#)]
- [15] Hyun-Seung Kim et al., "An Indoor Visible Light Communication Positioning System Using a RF Carrier Allocation Technique," *Journal of Lightwave Technology*, vol. 31, no. 1, pp. 134-144, 2013. [[CrossRef](#)] [[Google Scholar](#)] [[Publisher Link](#)]
- [16] Vaishali et al., "Lambertian Luminous Intensity Radiation Pattern Analysis in OLOS Indoor Propagation for Better Connectivity," *Wireless Communications and Mobile Computing*, vol. 2022, no. 1, pp. 1-11, 2022. [[CrossRef](#)] [[Google Scholar](#)] [[Publisher Link](#)]

- [17] Faisal Masood et al., "A Review of Recent Developments and Applications of Compound Parabolic Concentrator-Based Hybrid Solar Photovoltaic/Thermal Collectors," *Sustainability*, vol. 14, no. 9, pp. 1-31, 2022. [[CrossRef](#)] [[Google Scholar](#)] [[Publisher Link](#)]
- [18] Satea Hikmat Alnajjar, and Ahmed Majid Hameed, "Light Fidelity Performance via Hybrid Free Space Optic/Fiber Optic Communication under Atmospheric Disturbance," *Indonesian Journal of Electrical Engineering and Computer Science*, vol. 27, no. 1, pp. 355-365, 2022. [[CrossRef](#)] [[Google Scholar](#)] [[Publisher Link](#)]
- [19] Muhammad Shahin Uddin et al., "Mitigation Technique for Receiver Performance Variation of Multi-Color Channels in Visible Light Communication," *Sensors*, vol. 11, no. 6, pp. 6131-6144, 2011. [[CrossRef](#)] [[Google Scholar](#)] [[Publisher Link](#)]
- [20] Taegyoo Woo, Jong Kang Park, and Jong Tae Kim, "Effects of Incident Angle and Distance on Visible Light Communication," *International Journal of Electronics and Communication Engineering*, vol. 11, no. 1, pp. 70-73, 2017. [[Google Scholar](#)] [[Publisher Link](#)]
- [21] Yonghe Zhu et al., "Indoor Non-Line of Sight Visible Light Communication with a Bi-LSTM Neural Network," *2020 IEEE International Conference on Communications Workshops (ICC Workshops)*, Dublin, Ireland, pp. 1-6, 2020. [[CrossRef](#)] [[Google Scholar](#)] [[Publisher Link](#)]
- [22] M.S.M. Gismalla, and M.F.L. Abdullah, "Optimization of Received Power and SNR for an Indoor Attocells Network in Visible Light Communication," *Journal of Communications*, vol. 14, no. 1, pp. 64-69, 2019. [[Google Scholar](#)] [[Publisher Link](#)]